Characteristics of Competitive Adsorption between 2-Methylisoborneol and Natural Organic Matter on Superfine and Conventionally Sized Powdered Activated Carbons

Yoshihiko Matsui[1]*, Tomoaki Yoshida[2], Soichi Nakao[2], Detlef R. U. Knappe[3] and Taku Matsushita[1]

1 Faculty of Engineering, Hokkaido University, N13W8, Sapporo 060-8628, Japan.

2 Graduate School of Engineering, Hokkaido University, N13W8, Sapporo 060-8628, Japan.

3 Department of Civil, Construction, and Environmental Engineering, North Carolina State University, Raleigh, North Carolina 27695-7908, USA.

* Corresponding Author: Phone & Fax: +81-11-706-7280, E-mail: matsui@eng.hokudai.ac.jp.

ABSTRACT

When treating water with activated carbon, natural organic matter (NOM) is not only a target for adsorptive removal but also an inhibitory substance that reduces the removal efficiency of trace compounds, such as 2-methylisoborneol (MIB), through adsorption competition. Recently, superfine (submicron-sized) activated carbon (SPAC) was developed by wet-milling commercially available powdered activated carbon (PAC) to a smaller particle size. It was reported that SPAC has a larger NOM adsorption capacity than PAC because NOM mainly adsorbs close to the external adsorbent particle surface (shell adsorption mechanism). Thus, SPAC with its larger specific external surface area can adsorb more NOM than PAC. The effect of higher NOM uptake on the adsorptive removal of MIB has, however, not been investigated. Results of this study show that adsorption competition between NOM and MIB did not increase when NOM uptake increased due to carbon size reduction; i.e., the increased NOM uptake by SPAC did not result in a decrease in MIB adsorption capacity beyond that obtained as a result of NOM adsorption by PAC. A simple estimation method for determining the adsorbed amount of competing NOM (NOM that reduces MIB adsorption) is presented based on the simplified equivalent background compound (EBC) method. Furthermore, the mechanism of adsorption competition is discussed based on results obtained with the simplified EBC method and the shell adsorption mechanism. Competing NOM, which likely comprises a small portion of NOM, adsorbs in internal pores of activated carbon particles as MIB does, thereby reducing the MIB adsorption capacity to a similar extent regardless of adsorbent particle size. SPAC application can be advantageous because enhanced NOM removal does not translate into less effective removal of MIB. Molecular size distribution data of NOM suggest that the competing NOM has a molecular weight similar to that of the target compound.

KEYWORDS

PAC; particle size; sub-micrometer; competitive adsorption; humic substance; taste and odor

INTRODUCTION

2-methylisoborneol (MIB) is an earthy-musty odor compound that causes frequent customer complaints because it deteriorates the organoleptic qualities of drinking water. A widely accepted means for removing MIB is the addition of powdered activated carbon (PAC) prior to solid-liquid separation. MIB is a hydrophobic compound (log K_{ow} = 3.31) with small molecular size (molecular weight = 168) and is therefore efficiently adsorbed on activated carbon if it is present as a single compound in pure water. However, MIB always coexists with natural organic matter (NOM) in drinking water sources. Because NOM also adsorbs on activated carbon, it reduces the MIB adsorption capacity by competing for adsorption sites (direct site competition) and/or by hindering diffusion of MIB into carbon pores (pore blockage/constriction). NOM is also targeted for removal by many utilities because it is a precursor material for disinfection byproducts. Therefore, activated carbons that are effective for the simultaneous removal of MIB and NOM are desirable.

NOM can dramatically reduce the adsorption capacity of a micropollutant, but a micropollutant does not affect the adsorption of NOM because the concentration of NOM (mg/L) is several orders of magnitude higher than the concentration of most micropollutants including odor compounds (MIB), pesticides, and PPCPs (pharmaceuticals and personal care products), which occur at ng/L to μg/L levels. The competitive effect, namely the magnitude of the decrease in micropollutant adsorption capacity, is dependent on the loading of NOM on the carbon (Kilduff et al., 1998, Kilduff and Karanfil, 2002). Direct competition is the dominant mechanism at low NOM loading while pore blockage/constriction becomes important at high NOM loading (Kilduff et al., 1998, Matsui et al., 2003, Ding et al., 2006). It was shown that NOM of low molecular weight (MW) exerts a strong competitive effect on micropollutant adsorption (Newcombe et al., 1997, Hepplewhite et al., 2004, Kilduff et al., 1998, Newcombe et al., 2002b, Matsui 2002). Low MW NOM is adsorbed to a greater

66 extent than higher MW NOM (Matsui et al., 1993, Kilduff et al., 1996, Matsui 1998, Newcombe et al.,
67 2002a). The resulting higher loading of low MW NOM likely exerts a greater competitive effect on
68 micropollutant adsorption. However, even at the same loading, low MW NOM reduces micropollutant
69 adsorption to a greater degree than high MW NOM (Kilduff et al., 1998, Matsui et al., 2002), most
70 likely because low MW NOM can access the same adsorption sites on which micropollutants adsorb.

71 Although adsorption competition mechanisms between NOM and micropollutants are complex,
72 simple quantitative modeling approaches based on multi-component adsorption theory (i.e., ideal
73 adsorption solution theory) have been proposed and verified. One approach describing the adsorption
74 of a micropollutant from water containing NOM utilizes an equivalent background compound (EBC)
75 to approximate NOM (Najm et al., 1991) whereas another employs fictive components (Frick et al.,
76 1983, Crittenden et al., 1985). Based on the EBC approach, a simple relationship was found and
77 validated: the percentage of micropollutant removal that can be achieved with a given carbon dose in a
78 batch adsorption system is independent of the initial concentration of the micropollutant (Knappe et al.,
79 1998, Gillogly et al., 1998, Graham et al., 2000). This relationship holds when the micropollutant
80 concentration is low compared to the NOM concentration. In addition, the relationship is valid at
81 non-equilibrium conditions in both PAC and GAC adsorption processes (Matsui et al., 2001, 2002,
82 2003, Zoschke et al. 2011).

83 To help water treatment professionals choose effective activated carbons, many studies have been
84 conducted to better understand the mechanism of competition and to mathematically model the
85 competitive adsorption process. However, the increased knowledge seldom results in the production of
86 activated carbons that minimize the carbon usage rate. Some studies report enhancing the effectiveness
87 of activated carbon for MIB removal. In one such study, PACs were tailored by changing activation
88 conditions such that the PAC obtained with the optimized activation protocol outperformed
89 commercially available PAC (Tennant and Mazyck, 2003). Tailoring efforts were also conducted for

virgin and spent granular activated carbons to enhance their effectiveness for MIB removal (Nowack et al., 2004; Mackenzie et al., 2005). On the other hand, our research group proposed the use of superfine activated carbon (SPAC) with a particle size finer than that of traditional PAC, from which SPAC is produced by wet-milling. The design concept of SPAC was originally to improve the adsorbate uptake rate. In fact, SPAC is far superior to PAC in removing geosmin and NOM, especially at short contact times (Matsui et al., 2005, 2007, 2009). It was also found that SPAC has a higher NOM adsorption capacity than the parent PAC (Matsui et al., 2004, Ando et al., 2010). The higher NOM adsorption capacity of SPAC can be explained by the shell adsorption mechanism (SAM), which postulates that NOM molecules do not completely penetrate the adsorbent particle. Instead, they preferentially adsorb near the exterior particle surface (Ando et al., 2010, 2011, Matsui et al., 2011). As a result, a larger fraction of adsorption sites is accessible to NOM on SPAC compared to PAC due to the higher external surface area of the former. In the presence of NOM, geosmin and MIB adsorption capacities of SPAC did not become smaller than those of PAC even though NOM adsorbed to a greater extent on SPAC than on PAC (Matsui et al., 2010). This result suggests that the adsorption competition is less severe for SPAC than for PAC. However, the competitive mechanism was not inferred.

In this paper, adsorption equilibrium data of MIB and NOM were collected for SPAC and PAC and analyzed with the EBC and SAM models to elucidate differences in the mechanism of adsorption competition between MIB and NOM on PAC and SPAC.

METHODS

Activated carbon

Commercially available PAC (wood-based thermally activated carbon, Taikou-W, Futamura Chemical Industries Co., Gifu, Japan) was obtained in 2008 and 2010 and prepared as a slurry in ultrapure water. PAC was pulverized into SPAC with a wet bead mill (Metawater Co., Tokyo, Japan). In this paper, we refer to the as-received PAC obtained in 2008 as PAC08 and that obtained in 2010 as PAC10. The superfine carbons are referred to in a similar way as SPAC08 and SPAC10. Carbon properties are summarized in Table 1S (supplementary information) and the paper of Ando et al. (2010). In supplementary experiments we also used carbons that were pulverized such that median diameters were intermediate to those listed in Table 1S. Carbons were stored as slurries in ultrapure water at 4 °C and used after dilution and placement under vacuum. Particle size distributions of activated carbons were determined with a laser-light scattering instrument following the addition of a dispersant (0.02 mL of 18% anionic surfactant solution per 200 mL SPAC/PAC sample suspension containing between 0.001 and 0.01% carbon) and 4-min. sonification with ultrasound (LA-700, Horiba, Ltd., Kyoto, Japan).

Water samples

Waters containing NOM were collected from three lakes and one river in Japan (Table 2S). Samples were transported in polyethylene tanks and stored at 4°C. Waters were filtered through a 0.2-μm pore size membrane (DISMIC-25HP; Toyo Roshi Kaisha, Ltd., Tokyo) and adjusted to a similar DOC concentration of ~1.5 mg-C/L by dilution with ultrapure water (Milli-Q Advantage, Millipore Co.) amended with salts to obtain a uniform ionic composition. Salt additions were selected such that the highest ion concentration in each of the NOM-containing waters was reached in all waters. In addition, SFA and SHA waters were prepared by dissolving Suwannee River humic and fulvic acids in ultrapure water amended with inorganic ions to simulate the ionic composition of the diluted natural waters (Table S2).

137 Stock solutions of MIB were prepared by dissolving pure MIB (Wako Pure Chemical Industries, Ltd.,
138 Osaka, Japan) in ultrapure water (Milli-Q Advantage, Millipore Co.). NOM-containing waters were
139 spiked with the MIB stock solution to obtain an initial MIB concentration of ~1 μg/L (6 nmol/L). For
140 single-solute MIB experiments, the MIB stock solution was added to organic-free water (OFW)
141 amended with inorganic ions such that the ionic composition was similar to that of the diluted
142 NOM-containing waters (Table 2S). All waters were filtered through a 0.2-μm pore size membrane
143 before use. MIB concentrations were analyzed using a purge and trap concentrator coupled to a
144 GC-MS (GCMS-QP2010 Plus; Shimadzu Corp., Kyoto, Japan; Aqua PT 5000 J, GL Sciences Inc.,
145 Tokyo, Japan).

146 Dissolved organic carbon (DOC) served as a parameter for quantifying bulk NOM concentrations
147 (Model 810; Sievers Instruments, Inc., Boulder, CO, USA). Ultraviolet absorbance at 260 nm (UV_{260})
148 served as an indicator of chromophoric NOM (Model UV-240, Shimadzu Corp., Kyoto, Japan). MW
149 distributions of NOM were determined using high performance size exclusion chromatography
150 (HPSEC) [HP1100 (Agilent Technologies, Inc., CA, USA); packed column GL-P252 (Hitachi, Ltd.);
151 eluent: 0.02 M Na_2HPO_4 + 0.02 M KH_2PO_4]. Polystyrene sulfonate (weight-average MW 1920, 5180,
152 and 6130 Da) and salicylic acid (138 Da) were used for calibration (Zhou et al., 2000). The UV_{260}
153 absorbance and DOC (Model 810 Turbo; GE Analytical Instruments) of the HPSEC column effluent
154 were measured continuously.

155

156 **Batch adsorption tests**

157 In adsorption equilibrium tests, aliquots (150 mL) of OFW or NOM-containing water spiked with MIB
158 (C_0 = ~1 μg/L) were transferred to 160-mL vials. A specified amount of SPAC/PAC was immediately
159 added, the vials were manually shaken and then agitated on a mechanical shaker for one week at a

160 constant temperature of 20°C. In a preliminary experiment, it was confirmed that MIB adsorption
161 equilibrium was reached in one week and that NOM adsorption equilibrium was almost reached.
162 Control tests were also conducted by using multiple bottles that did not contain carbon to confirm that
163 MIB and NOM concentration changes during long-term mixing were negligible. After filtering water
164 samples through a 0.2-μm membrane filter, adsorbate (MIB and NOM) concentrations in the aqueous
165 phase were measured. Solid-phase concentrations of each adsorbate were calculated from the mass
166 balance.

167

168 **RESULTS AND DISCUSSION**

169

170 **MIB adsorption capacities on S-PAC and PAC**

171 MIB adsorption isotherm experiments were conducted in OFW and in 10 waters containing NOM. For
172 all tested carbons, MIB adsorption capacities were smaller in NOM-containing waters than in OFW
173 (Figure 1S, supplementary information). In OFW, the MIB adsorption capacity of SPAC was slightly
174 higher than that of PAC, but this difference was small (e.g., <30% at an aqueous-phase concentration
175 of 0.6 nmol/L = 100 ng/L). In contrast, the MIB adsorption capacity in NOM-containing waters was
176 only 10-40% of that obtained in OFW. Because OFW contained a similar ionic composition as the
177 NOM-containing waters and the only difference between NOM-containing water and OFW was the
178 presence/absence of NOM, the lower MIB adsorption capacity in NOM-containing waters should be
179 due to adsorption competition by NOM. The ratio of the MIB adsorption capacity in NOM-containing
180 water to that in OFW at an equilibrium aqueous-phase concentration of 0.6 nmol/L (= 100 ng/L,
181 approximately the median concentration in the data, Figure 1S) is summarized in Figure 1 (values
182 calculated from each Freundlich isotherm model fit). All experiments in NOM-containing waters were

conducted at nearly the same initial NOM concentration, but the effect of NOM on MIB adsorption differed among the NOM-containing waters. The reduction in MIB adsorption capacity was higher for the NOM in Kasumigaura and Hakucho waters and lower for the NOM in Inba and Chibaberi waters. Furthermore, results in Figure 1 show that the effect of NOM on the reduction in MIB adsorption capacity was similar for PAC and SPAC for 9 out of 10 experiments.

In experiments evaluating MIB adsorption in NOM-containing waters, aqueous-phase DOC concentrations were also measured. At a fixed carbon dose of 8 mg/L, which roughly yielded an equilibrium MIB concentration of 100 ng/L, DOC loadings on SPAC were 1.6 to 3.9 times those obtained with PAC (Figure 2S, Figure 3S). Similarly, DOC loadings were compared at a given equilibrium aqueous-phase MIB concentration of 100 ng/L (Figure 2). DOC loadings were obtained from each Freundlich model fit to DOC isotherm data (q_{DOC} vs. C_{DOC}) at a carbon dose that yielded an equilibrium aqueous-phase MIB concentration of 100 ng/L. DOC loadings varied greatly among NOM sources and were consistently higher on SPAC than on PAC. DOC loadings ranged from 60 to 135 mg-C/g for SPAC and from 21 to 46 mg-C/g for PAC. In Kasumigaura water, DOC loadings were relatively low (Figure 2), but the MIB adsorption capacity was more strongly affected than in other NOM-containing waters (Figure 1). In contrast, Inba water yielded a higher DOC loading on both PAC and SPAC, but the effect on MIB loading was not as strong as that obtained in Kasumigaura water. Therefore, the DOC loading on the carbon is not indicative of the NOM effect on MIB adsorption capacity, and the NOM competing with MIB is likely only a fraction of the total NOM.

Analysis of competitive adsorption by equivalent background compound method

To distinguish between adsorption of (1) NOM and (2) the NOM fraction that directly competes with MIB for adsorption sites, an equivalent background compound (EBC) adsorption analysis was conducted. When competing NOM is represented by a single hypothetical compound (EBC), the

system containing MIB and NOM can be modeled as a bi-solute system. Incorporating the Freundlich isotherm equation into the bi-solute form of the Ideal Adsorption Solution Theory, the MIB adsorption isotherm becomes

$$C_M = \frac{q_M}{q_M + q_E}\left(\frac{n_M q_M + n_E q_E}{n_M K_M}\right)^{n_M} \quad (1)$$

where, C_M is the liquid-phase concentration of MIB (nmol/L), q_M is the solid-phase concentration of MIB (nmol/mg), q_E is the solid-phase concentration of EBC (nmol/mg), n_M and K_M are the single-solute Freundlich isotherm exponent and constant for MIB [dimensionless and (nmol/mg)/(nmol/L)$^{1/n}$, respectively], and n_E is the single-solute Freundlich isotherm exponent for the EBC (dimensionless).

With the two assumptions that (1) the EBC solid-phase concentration was much greater than the solid-phase concentration of the target compound and (2) the Freundlich exponents $1/n_M$ and $1/n_E$ are not very different, i.e., both fall into the range 0.1-1, Knappe et al. (1998) derived an equation that validated the experimentally observed direct proportionality between MIB adsorption capacity and initial MIB concentration at a given carbon dose. With the same assumptions, equation (1) becomes;

$$q_E{}^* \equiv q_E n_E^{\frac{n_M}{n_M - 1}} = (n_M K_M)^{\frac{n_M}{n_M - 1}}\left(\frac{C_M}{q_M}\right)^{\frac{1}{n_M - 1}} \quad (2)$$

where, $q_E{}^*$ is the pseudo solid-phase concentration for the competing NOM fraction (nmol/mg).

Equation (2) illustrates that the EBC loading (q_E) can be quantitatively estimated if C_M, q_M, n_M, K_M, and n_E are known. C_M and q_M values were obtained from MIB adsorption isotherm experiments in NOM-containing waters, and $1/n_M$ and K_M values were obtained from Freundlich model fits to MIB adsorption isotherm data obtained in OFW [Figure 1S and Table 3S (supplementary information)]. The value of $1/n_E$, Freundlich exponent of EBC, was unknown. However, the value of $q_E{}^*$ defined by

equation (2) can be used for comparing EBC loadings on the carbons if $1/n_E$ and $1/n_M$ values are similar among carbons. Similarity in $1/n_M$ values is demonstrated in Table 3S, and similarity in $1/n_E$ has been demonstrated in a previous study that evaluated the effects of NOM on MIB adsorption by four activated carbons (Newcombe et al. 2002b). The EBC loading (q_E) is linked to q_E^* via the term $n_E^{\frac{n_M}{n_M-1}}$, which ranges in magnitude from 3.95 to 4.67 if $1/n_E = 0.47$ (Table 1) and $1/n_M$ ranges from 0.45 to 0.51 (Table 3S). In that case, q_E is 21.4-25.3% of the q_E^* values calculated from the right hand side of equation 2.

In this study, the loading of the competing NOM fraction was estimated by calculating q_E^*. The magnitude of the pseudo-concentration decrease of the competing NOM fraction (ΔC_E^*) can be calculated from

$$\Delta C_E^* \equiv C_{E,0}^* - C_E^* = C_C q_E^* \qquad (3)$$

where C_E^* ($= C_E n_E^{\frac{n_M}{n_M-1}}$) is the pseudo aqueous-phase concentration of the competing NOM fraction (nmol/L), $C_{E,0}^*$ is the initial pseudo aqueous-phase concentration of the competing NOM fraction (nmol/L), and C_C is the carbon dose (mg/L).

At high carbon doses, $C_E << C_{E,0}$ and $C_M << C_{M,0}$ ($C_{E,0}$ and $C_{M,0}$ are initial EBC and MIB concentrations, respectively). As a result, an isotherm for the micropollutant in natural water becomes parallel to the single-solute isotherm of the trace organic compound on a log-log scale plot between solid- and liquid-phase concentrations (Knappe 1996; Qi et al., 2007). Therefore, the isotherm for MIB in natural water can be described by a pseudo-single solute isotherm equation with the same Freundlich exponent as that obtained for the single-solute MIB system;

$$q_M = K_M^* C_M^{\frac{1}{n_M}} \qquad (4)$$

where, K_M^* is the Freundlich constant describing the MIB adsorption isotherm obtained in

246 NOM-containing water [(nmol/mg)/(nmol/L)$^{1/n}$].

247 By substituting equation (4) into (2), equation (2) becomes;

$$q_E{}^* = q_M \left(n_M \frac{K_M}{K_M{}^*} \right)^{\frac{n_M}{n_M - 1}} \qquad (5)$$

248 Therefore, once K_M and n_M are known, $q_E{}^*$ values can be calculated for a given carbon dose from
249 equation (5) after determining q_M at a given carbon dose from the mass balance (eq. 6) and $K_M{}^*$ from
250 equation (4).

$$C_{M,0} - C_M = C_C q_M \qquad (6)$$

251 Pseudo solid-phase concentrations of the competing NOM fraction ($q_E{}^*$) and DOC (q_{DOC}) are
252 compared in Figure 3. For $q_E{}^*$, values decreased with increasing carbon dose. Corresponding $\Delta C_E{}^*$
253 values increased initially with carbon dosage and plateaued at a carbon dosage of ~10 mg/L. On the
254 other hand, ΔC_{DOC} continued to increase with increasing carbon dose even after $\Delta C_E{}^*$ values had
255 plateaued. This observation suggests that the competing NOM fraction is a strongly adsorbing NOM
256 fraction that preferentially adsorbs on carbon and is almost completely removed with relatively low
257 carbon doses. Furthermore, values of $q_E{}^*$ were similar between SPAC and PAC while values of q_{DOC}
258 were higher on SPAC. This result directly relates to the experimental observations summarized in
259 Figures 1 and 2; i.e., DOC loadings are higher on SPAC than on PAC while reductions in MIB loading
260 resulting from the presence of NOM were similar for PAC and SPAC.

261 Figure 4 summarizes $q_E{}^*$ values corresponding to the MIB and DOC adsorption data shown in Figures
262 1 and 2 [$q_E{}^*$ values at a carbon dose of 8 mg/L are shown in Figure 4S (supplementary information)].
263 Values of $q_E{}^*$ were similar between SPAC and PAC for all tested waters, which clearly indicates that
264 SPAC adsorbed the competing NOM fraction to a similar extent as PAC. In terms of adsorption of
265 competing NOM, therefore, SPAC and PAC are not very different. However, SPAC adsorbed NOM to

a greater extent than PAC (Figure 2). These results mean that SPAC adsorbed non-competing NOM (NOM that is not competitive to MIB) more than PAC, but SPAC and PAC adsorbed similar amounts of competing NOM such that MIB adsorption was affected to a similar extent.

Adsorption of competing NOM

In Figure 3, ΔC_E^* values plateaued once the carbon dose reached about 10 mg/L. This means that the competing NOM fraction was almost completely taken up from solution at carbon doses >10 mg/L. Therefore, the ΔC_E^* value when C_C > 10 mg/L should be equivalent to the concentration of the competing NOM fraction initially present in the water before dosing carbon ($C_{E,0}^*$).

Figure 5 summarizes $C_{E,0}^*$ values for the different waters that were calculated with equations (3)-(6). $C_{E,0}^*$ values differed among the tested NOM sources (range: ~0.2 μmol/L for SHA08 to ~1.3 μmol/L for Hakucho08). However, $C_{E,0}^*$ values of a given water were almost the same between SPAC and PAC, which again shows that the competing NOM fraction is similar for SPAC and PAC.

For the waters having higher $C_{E,0}^*$ values (Hakucho and Kasumigaura waters), the difference in q_{DOC} values between SPAC and PAC was smaller than for other waters (Figure 2). In an analogous manner, the difference in q_{DOC} values between SPAC and PAC was larger for waters with lower $C_{E,0}^*$ values (e.g., SHA and SFA waters). Ando et al. (2010, 2011) reported that the increase in DOC adsorption capacity with decreasing carbon size is due to the limited penetration distance of NOM from the exterior surface of carbon particles (shell adsorption mechanism). The specific external surface area (surface area per unit mass) available for adsorption is therefore greater for smaller adsorbent particles, and hence the DOC adsorption capacity of SPAC, which has a smaller particle size than PAC, is larger.

If adsorption occurred only at the external particle surface, then the increase in DOC adsorption capacity would be inversely proportional to adsorbent particle size (i.e., the slope of log solid-phase concentration when plotted as a function of log median diameter would equal −1). In contrast, a slope of zero would indicate that DOC adsorption occurs uniformly throughout the entire carbon particle. Matsui et al. (2011) reported, however, that slope values fell between 0 and −1, indicating that a fraction of the interior region of the adsorbent particles is available for DOC adsorption. In this study, the magnitude of the inverse of the slope (i.e. gradient of log D_{50} / log q_{DOC}) is called the penetration index.

The dependence of the solid-phase DOC concentration (q_{DOC}) on median carbon diameter (D_{50}) is shown on a log-log scale in Figure 5S (supplementary information). DOC isotherms were modeled by the Freundlich isotherm equation, as shown in Figure 3S, and q_{DOC} values for Figure 5S were calculated for the carbon dose, at which 50% of the initial aqueous-phase DOC concentration was adsorbed (Ando et al., 2010). The correlations in Figure 5S are fairly strong with coefficients of determination ranging from 0.84 to 1.00. Slope values ranged from -0.27 to -0.62 (Figure 5S), illustrating that NOM accessed a substantial fraction of the interior region of the adsorbent particles. The absolute value of the inverse of an exponent shown in Figure 5S represents the penetration index for a given NOM. When the penetration index values were plotted against $C_{E,0}{}^{*}$ (Figure 6), a fairly good correlation was obtained ($r^2 = 0.56$). NOM-containing waters with a high initial concentration of competing NOM (represented by $C_{E,0}{}^{*}$), such as Kasumigaura water, had a large penetration index. A large penetration index value indicates that NOM molecules can access a large fraction of the interior region of adsorbent particles. Therefore, the correlation shown in Figure 6 suggests that NOM molecules that are able to access the interior region of adsorbent particles to a greater extent exert a greater degree of adsorption competition. Small penetration index values, on the other hand, indicate that NOM principally adsorbed close to the external particle surface and did not compete as strongly with MIB for adsorption sites. For such waters (e.g., SHA-08), $C_{E,0}{}^{*}$ and $q_{E}{}^{*}$ values are small.

313

314 **Characteristics of competing NOM**

315 Prior research has shown that the low-MW NOM fraction competes directly with strongly adsorbing
316 micropollutants (Newcombe et al., 1997, Hepplewhite et al., 2004, Kilduff et al., 1998, Newcombe et
317 al., 2002b, Matsui 2002). In this study, the fraction of NOM below a given target MW (MW_T) was
318 estimated from HPSEC data according to equations (7) and (8):

319 DOC of NOM with MW < MW_T = Initial DOC × Fraction (< MW_T in DOC MW chromatogram)

320 (7)

321 UV_{260} of NOM with MW < MW_T = Initial UV_{260} × Fraction (< MW_T in UV_{260} MW chromatogram)

322 (8)

323 Correlations between the NOM fraction with MW < MW_T and the initial pseudo aqueous-phase
324 concentration of the competing-NOM ($C_{E,0}^*$) were tested by changing MW_T. As shown in Figure 6S, a
325 fairly good correlation ($R^2 > 0.6$) was observed for UV_{260} when MW_T was 230 Da (Panel K).

326 The MW of the competing NOM was further estimated by using the gradients of the regression lines in
327 Figure 6S. In Figure 6S, $C_{E,0}^*$ (x-axis value) is the molar concentration of the competing NOM
328 multiplied by $n_E^{\frac{n_M}{n_M-1}}$, and is obtained from equations (3)-(6) while y-axis values are carbon mass
329 concentration (DOC, mg-C/L) or UV absorbance (UV_{260}, m^{-1}). Therefore,

$$\text{Gradient } (\text{DOC}/C_{E,0}^*) = \frac{\text{Carbon content} \times \text{MW}}{n_E^{\frac{n_M}{n_M-1}}} \quad (9)$$

$$\text{Gradient } (UV_{260}/C_{E,0}{}^{*}) = \frac{\text{SUVA} \times \text{Carbon content} \times \text{MW}}{n_E{}^{\frac{n_M}{n_M-1}}} \qquad (10)$$

When SUVA (specific UV absorbance), carbon content, n_E for the competing NOM fraction, and n_M for MIB are known, the MW of the competing NOM fraction can be estimated from equations (9) and (10). Using the values shown in Table 1 and an average value for n_M (0.47, Table 3S) resulted in the MW estimates shown in each panel of Figure 6S. For example, the correlation in Panel A was obtained by assuming that the MW of competing NOM fraction was less than 2 kDa (MW_T = 2 kDa). However, the resulting regression line indicates that the MW of the competing NOM was 10 kDa for n_E of 0.47 (6.4 kDa for n_E of 0.6 and 51 kDa for n_E of 0.2); thus, consistency was not obtained between MW_T and the MW value resulting from the slope. Consistency in MW as well as a good correlation was observed for UV_{260} when MW_T was 230 Da (Figure 7, Panel K of Figure 6S). The regression line indicates the MW is 180 Da for n_E of 0.47 (110 Da for n_E of 0.6 and 900 Da for n_E of 0.2). Because this MW value is close to that of MIB (168 Da), it is highly likely that the competing NOM has a similar molecular size as the targeted micropollutant. Assuming a MW of 180 Da, competing NOM concentrations were estimated from $C_{E,0}{}^{*}$ to range from 3 to 30 μg-C/L for the different NOM-containing waters. This result suggests that the competing NOM represents only 0.2 to 2% of entire NOM.

CONCLUSIONS

SPAC more effectively adsorbed NOM than PAC at a given carbon dose. However, the higher NOM loading on SPAC did not reduce the MIB adsorption capacity more, relative to organic-free water, than the lower NOM loading on PAC. By using the simplified EBC method and MW distribution data of NOM, it was estimated that the competing NOM fraction (1) contains UV-absorbing moieties, (2) has a MW <230 Da, and (3) constitutes only 0.2 to 2% of the entire NOM. This NOM fraction competes with MIB for adsorption sites located in the interior region of carbon particles, and its solid-phase

concentration is not a function of carbon size (SPAC/PAC). On the other hand, the higher NOM loading on SPAC relative to PAC is a result of the adsorption of non-competing NOM on sites near the external surface of the carbon particle.

Acknowledgements

This study was supported by Grant-in-Aid for Scientific Research A(21246083) and S (24226012) from the Japan Society for the Promotion of Science, by a research grant from the Ministry of Health, Labour and Welfare, and by Metawater Co., Tokyo, Japan.

Appendix. Supplementary Information

Table 1S–4S and Figures 1S–6S are available in the online version at ######.

References

Ando, N., Matsui, Y., Kurotobi, R., Nakano, Y., Matsushita, T., Ohno, K. (2010) Comparison of natural organic matter adsorption capacities of super-powdered activated carbon and powdered activated carbon. Water Res 44(14), 4127-4136.

Ando, N., Matsui, Y., Matsushita, T., Ohno, K. (2011) Direct observation of solid-phase adsorbate concentration profile in powdered activated carbon particle to elucidate mechanism of high adsorption capacity on super-powdered activated carbon. Water Res. 45(2), 761-767.

Crittenden, J.C., Luft, P., Hand, D.W. (1985) Prediction of multicomponent adsorption equilibria in background mixtures of unknown composition. Water Res. 19(12), 1537–48.

373 Ding L., Marinas B.J., Schideman L.C., Snoeyink V.L., Li Q. 2006 Competitive effects of natural
374 organic matter: Parametrization and verification of the three-component adsorption model
375 COMPSORB. Environ. Sci. Technology 40(1), 350-356.

376 Frick, B.R., Sontheimer, H. (1983) Adsorption equilibria in multisolute mixtures of known and
377 unknown composition. In: Suffet, I.H., McGuire M.J., editors. *Treatment of Water by Granular*
378 *Activated Carbon*. Washington, DC, American Chemical Society, pp. 247–68.

379 Gillogly, T.E.T., Snoeyink, V.L., Elarde, J.R., Wilson, C.M., Royal, E.P. (1998) ^{14}C-MIB adsorption on
380 PAC in natural water. J. Am Water Works Assoc 90(1), 98–108.

381 Graham, M.R., Summers, R.S., Simpson, M.R., MacLeod, B.W. (2000) Modeling equilibrium
382 adsorption of 2-methylisoborneol and geosmin in natural waters. Water Res. 34(8), 2291-2300.

383 Hepplewhite, C., Newcombe, G., Knappe, D.R.U. (2004) NOM and MIB, who wins in the competition
384 for activated carbon adsorption sites? Water Sci. Tech. 49(9), 257-265.

385 Kilduff, J.E., Karanfil, T., Chin, Y., Weber, W.J. Jr. (1996). “Adsorption of natural organic
386 polyelectrolytes by activated carbon: A size-exclusion chromatography study.” Envir. Sci.
387 Technol., 30(4), 1336-1343.

388 Kilduff J.E., Karanfil T., Weber Jr. W.J. 1998 TCE adsorption by GAC preloaded with humic
389 substances. Jour. Amer. Water Works Assoc. 90: 76-89.

390 Kilduff, J.E., Karanfil, T. (2002) Trichloroethylene adsorption by activated carbon preloaded with
391 humic substances: effects of solution chemistry . Water Res. 36(7), 1685-1698.

392 Knappe, D.R.U. (1996) Predicting the Removal of Atrazine by Powdered and Granular Activated
393 Carbon. Doctoral Thesis, University of Illinois, Urbana, IL.

394 Knappe, D.R.U., Matsui, Y., Snoeyink, V.L., Roche, P., Prados, M.J., Bourbigot, M.M. (1998)
395 Predicting the Capacity of Powdered Activated Carbon for Trace Organic Compounds in
396 Natural Waters. Environ. Sci. Technology 32(11), 1694-1698.

397 Mackenzie, J.A., Tennant, M.F., Mazyck, D.W. (2005) Tailored GAC for the effective control of
398 2-methylisoborneol. Journal American Water Works Association 97(6), 76-87.

399 Matsui, Y., Kamei, T., Tambo, N., Taniguchi, K. (1993). Classification of aquatic humic substances
400 and their activated carbon adsorbability. Journal Japan Soc. Water Environ. 16(7), 497-506 (in
401 Japanese).

402 Matsui, Y., Yuasa, A., Li, F. (1998) Overall Adsorption isotherm of natural organic matter. Journal
403 Environ. Eng. 124(11), 1099-1107.

404 Matsui, Y., Colas, F., Yuasa, A. (2001) Removal of synthetic organic chemical by powdered activated
405 carbon during ultrafiltration. II: model application. Water Res. 35(2), 464-470.

406 Matsui, Y., Knappe, D.R.U., Iwaki, K., Ohira, H. (2002) Pesticide adsorption by granular activated
407 carbon adsorbers-2. effects of pesticide and natural organic matter characteristics on pesticide
408 breakthrough curves. Environ. Sci. Tech. 36(15), 3432-3438.

409 Matsui, Y., Fukuda, Y., Inoue, T. and Matsushita, T. (2003) Effect of natural organic matter on
410 powdered activated carbon adsorption of trace contaminants: characteristics and mechanism of
411 competitive adsorption. Water Res. 37(18), 4413-4424.

412 Matsui, Y., Fukuda, Y., Murase, R., Aoki, N., Mima, S., Inoue, T. and Matsushita, T. (2004) Micro-ground
413 powdered activated carbon for effective removal of natural organic matter during water treatment.
414 Water Sci. Tech.: Water Supply 4(4), 155–163.

415 Matsui Y, Murase R, Sanogawa T, Aoki H, Mima S, Inoue T, Matsushita T (2005) Rapid adsorption
416 pretreatment with submicrometre powdered activated carbon particles before microfiltration.
417 Water Sci. Technology 51(6-7), 249-256.

418 Matsui, Y., Aizawa, T., Kanda, F., Nigorikawa, N., Mima, S., Kawase, Y. (2007). Adsorptive removal of
419 geosmin by ceramic membrane filtration with super-powdered activated carbon. Journal Water
420 Supply Res. Tech.-Aqua 56(6–7), 411-418.

421 Matsui, Y., Ando, N., Sasaki, H. , Matsushita, T., Ohno, K. (2009). Branched pore kinetic model analysis
422 of geosmin adsorption on super-powdered activated carbon. *Water Res.* **43**(12), 3095-3103.

423 Matsui, Y., Nakano, Y., Ando, N., Sasaki, H., Ohno, K., Matsushita, T. (2010) Geosmin and
424 2-methylisoborneol adsorption on super-powdered activated carbon in the presence of natural
425 organic matter. Water Sci. Tech. 62(11), 2664-2668.

426 Matsui, Y., Ando, N., Yoshida, T., Kurotobi, R., Matsushita, T., Ohno, K. (2011) Modeling high
427 adsorption capacity and kinetics of organic macromolecules on super-powdered activated carbon.
428 Water Res. 45, 1720-1728.

429 Motulsky, H.J., Christopoulos, A. (2004) Fitting models to biological data using linear and nonlinear
430 regression: A practical guide to curve fitting. Oxford University Press.

431 Najm, I.N., Snoeyink, V.L., Richard, Y. (1991) Effect of initial concentration of a SOC in natural water on
432 its adsorption by activated carbon. Journal American Water Works Association 83(8), 57–63.

433 Newcombe, G., Drikas, M., Hayes, R. (1997) Influence of characterised natural organic material on
434 activated carbon adsorption: 2. effect on pore volume distribution and adsorption of
435 2-methylisoborneol. Water Rese. 31(5), 1065-1073.

436 Newcombe, G., Morrison, J., Hepplewhite, C. (2002a) Simultaneous adsorption of MIB and NOM

437 onto activated carbon. I. characterisation of the system and NOM adsorption . Carbon 40(12),
438 2135-2146.

439 Newcombe, G., Morrison, J., Hepplewhite, C., Knappe, D.R.U. (2002b) Simultaneous adsorption of
440 MIB and NOM onto activated carbon - II. competitive effects. Carbon 40(12), 2147-2156.

441 Nowack, K.O., Cannon, F.S., Mazyck, D.W. (2004) Enhancing activated carbon adsorption of
442 2-methylisoborneol: methane and steam treatments. Environ. Sci. Tech. 38(1), 276–284.

443 Qi, S., Schideman, L., Mariñas, B.J., Snoeyink, V.L., Campos, C. (2007) Simplification of the IAST
444 for activated carbon adsorption of trace organic compounds from natural water. Water Res.
445 41(2), 440-448.

446 Tennant, M.F., Mazyck, D.W. (2003) Steam-pyrolysis activation of wood char for superior odorant
447 removal. Carbon 41(12), 2195–2202

448 Worch, E. (2010) Competitive adsorption of micropollutants and NOM: a comparative study of
449 different model approaches. Journal Water Supply Res. Tech.-AQUA 59 (5), 285–297.

450 Zoschke, K., Engel, C., Börnick, H., Worch, E. (2011) Adsorption of geosmin and 2-methylisoborneol
451 onto powdered activated carbon at non-equilibrium conditions: Influence of NOM and process
452 modeling. Water Res. 45(15), 4544-4550.

453 Zhou, Q., Cabaniss, S.E., Maurice, P.A. (2000) Considerations in the use of high-pressure size
454 exclusion chromatography (HPSEC) for determining molecular weights of aquatic humic
455 substances. Water Res. 34(14), 3505-3514.

456

Table and figure and captions

Table 1. Parameter values of equations (9) and (10)

Figure 1. Ratio of MIB adsorption capacity in NOM-containing water to that in OFW. MIB adsorption capacities were evaluated from batch adsorption isotherm data at an equilibrium MIB aqueous-phase concentration of 0.6 nmol/L (100 ng/L).

Figure 2. DOC loadings on each carbon at experimental conditions matching those described for Figure 1.

Figure 3. Pseudo solid-phase concentrations of the competing NOM fraction (q_E^*) and the corresponding pseudo aqueous-phase concentration decrease (ΔC_E^*) as a function of carbon dose (left panel). DOC loadings (q_{DOC}) and corresponding aqueous-phase concentration decreases (ΔC_{DOC}) as a function of carbon dose (left panel). Results shown are for SFA-10 water. Data points in the left panel were obtained from equation (2) using experimental MIB adsorption isotherm data. The lines in the left panel were obtained from equations (3)-(6) and the parameter values shown in Tables 3S and 4S (supplementary information). The plots in the right panel were obtained from experimental DOC adsorption isotherm data. The lines in the right panel were obtained from corresponding Freundlich isotherm model fits.

Figure 4. Pseudo solid-phase concentration of the competing NOM fraction (q_E^*) at experimental conditions matching those described for Figure 1.

Figure 5. Initial pseudo aqueous-phase concentrations of competing NOM fractions ($C_{E,0}^*$) in the tested NOM-containing waters.

Figure 6 Relationship between penetration index (absolute value of gradient: log D_{50} / log q_{DOC}) and initial pseudo aqueous-phase concentration of the competing NOM fraction.

Figure 7. Relationship between the UV_{260} absorbance of NOM with a molecular weight smaller than 230 Da and the competing NOM concentration ($C_{E,0}^*$). UV_{260} absorbance values were obtained from size-exclusion chromatograms. $C_{E,0}^*$ values were estimated from MIB isotherms by using equations (3)-(6). Coefficients of determination (R^2) were determined from 1-SSreg/SStot, where SSreg is the sum of squares of the residuals around the regression line with an intercept of 0, and SStot is the sum of squares of the residuals around a horizontal line representing the mean absorbance value of the data shown (Motulsky and Christopoulos, 2004).

Table 1. Parameter values of equations (9) and (10)

Parameter	Value	
$1/n_E$	0.47	Assumed to be similar to that of MIB (the average value of n_M) (Knappe et al., 1998, Worch 2010)
	(0.2 ~ 0.6)	Possible range
SUVA	6.1 (m^{-1} L/mg-C)	Highest observed value (Table 2S)
Carbon content	0.52 (mg-C/mg)	The value for fulvic acid (International Humic Substance Society)

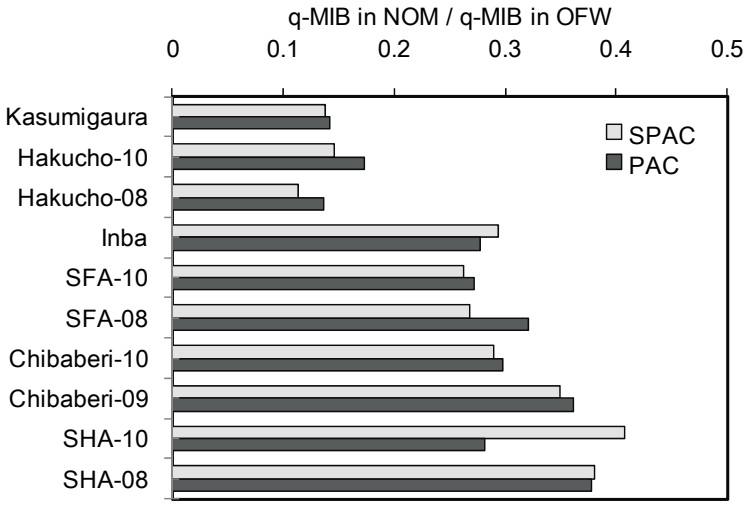

Figure 1. Ratio of MIB adsorption capacity in NOM-containing water to that in OFW. MIB adsorption capacities were evaluated from batch adsorption isotherm data at an equilibrium MIB aqueous-phase concentration of 0.6 nmol/L (100 ng/L).

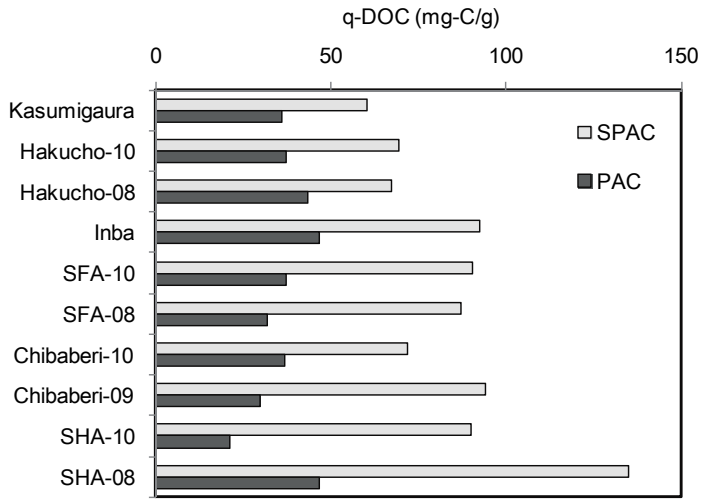

Figure 2. DOC loadings on each carbon at experimental conditions matching those described for Figure 1.

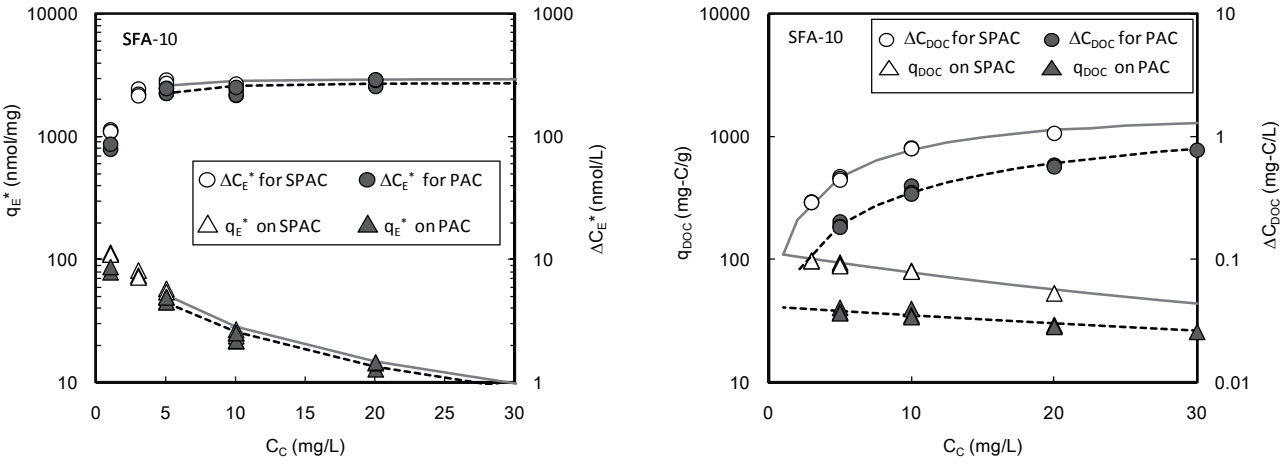

Figure 3. Pseudo solid-phase concentrations of the competing NOM fraction (q_E^*) and the corresponding pseudo aqueous-phase concentration decrease (ΔC_E^*) as a function of carbon dose (left panel). DOC loadings (q_{DOC}) and corresponding aqueous-phase concentration decreases (ΔC_{DOC}) as a function of carbon dose (left panel). Results shown are for SFA-10 water. Data points in the left panel were obtained from equation (2) using experimental MIB adsorption isotherm data. The lines in the left panel were obtained from equations (3)-(6) and the parameter values shown in Tables 3S and 4S (supplementary information). The plots in the right panel were obtained from experimental DOC adsorption isotherm data. The lines in the right panel were obtained from corresponding Freundlich isotherm model fits.

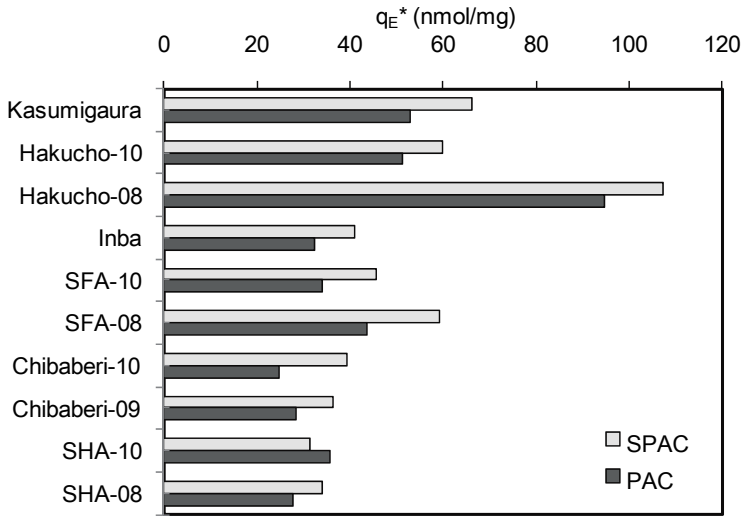

Figure 4. Pseudo solid-phase concentrations of the competing NOM fraction (q_E^*) at experimental conditions matching those described for Figure 1.

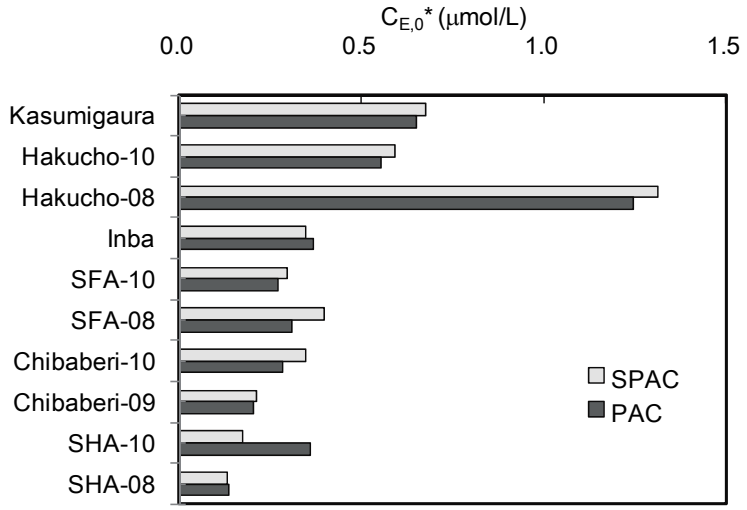

Figure 5. Initial pseudo aqueous-phase concentrations of competing NOM fractions ($C_{E,0}^{*}$) in the tested NOM-containing waters.

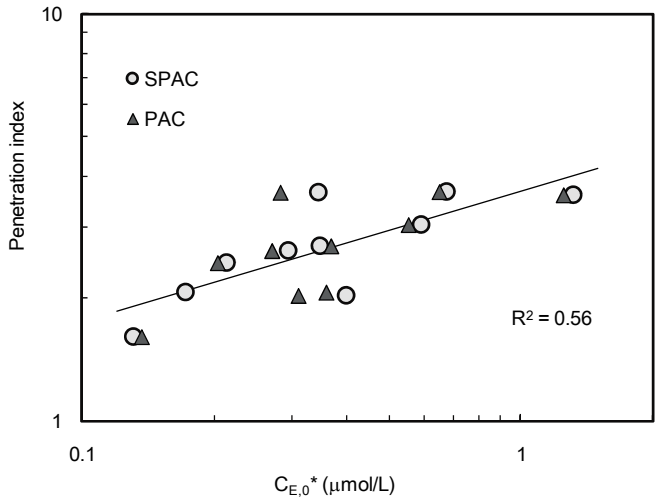

Figure 6. Relationship between penetration index (absolute value of gradient: log D_{50} / log q_{DOC}) and initial pseudo aqueous-phase concentration ($C_{E,0}^{*}$) of the competing NOM fraction.

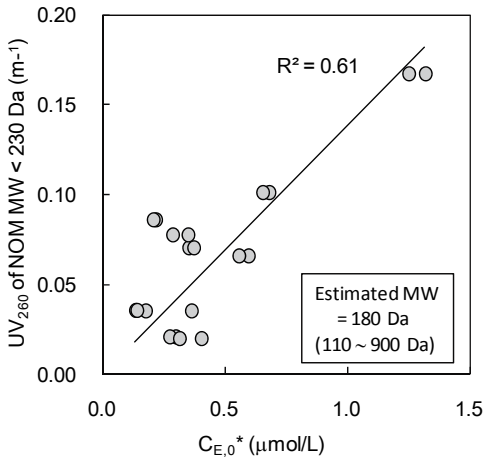

Figure 7. Relationship between the UV_{260} absorbance of NOM with a molecular weight smaller than 230 Da and the competing NOM concentration ($C_{E,0}^{*}$). UV_{260} absorbance values were obtained from size-exclusion chromatograms. $C_{E,0}^{*}$ values were estimated from MIB isotherms by using equations (3)-(6). Coefficients of determination (R^2) were determined from 1-SSreg/SStot, where SSreg is the sum of squares of the residuals around the regression line with an intercept of 0, and SStot is the sum of squares of the residuals around a horizontal line representing the mean absorbance value of the data (Motulsky and Christopoulos, 2004).

Supplementary Information

Characteristics of Competitive Adsorption between 2-Methylisoborneol and Natural Organic Matter on Superfine and Conventionally Sized Powdered Activated Carbons

Yoshihiko Matsui[1*], Tomoaki Yoshida[2], Soichi Nakao[2], Detlef R. U. Knappe[3] and Taku Matsushita[1]
1 Faculty of Engineering, Hokkaido University, N13W8, Sapporo 060-8628, Japan.
2 Graduate School of Engineering, Hokkaido University, N13W8, Sapporo 060-8628, Japan.
3 Department of Civil, Construction, and Environmental Engineering, North Carolina State University, Raleigh, North Carolina 27695-7908, USA.
*** Corresponding Author: Phone & Fax: +81-11-706-7280, E-mail: matsui@eng.hokudai.ac.jp.**

Table 1S. Size and surface area of activated carbon particles

	Median diameter (D_{50}, μm)	Effective diameter (D_{10}, μm)	BET surface area (m^2/g)
PAC-08	8.12	2.48	1090
SPAC-08	0.66	0.23	1170
PAC-10	13.5	3.35	1070
SPAC-10	0.86	0.4	1130

Table 2S. Characteristics of test solutions (DOC, UV_{260}, and MIB concentrations were measured for blank bottles in adsorption isotherm tests. Ionic concentrations represent target concentrations).

Sample water	DOC	Weight-averaged MW of NOM	Number-averaged MW of NOM	UV_{260}	SUVA	MIB	Na^+	K^+	Ca^{2+}	Mg^{2+}	Cl^-	SO_4^{2-}	HCO_3^-	NO_3^-	Conductivity	Sources	Sampling date	Tested PAC
	mg/L	Da	Da	cm^{-1}	L/(mg·m)	μg/L	mM	mM	mM	mM	mM	mM	mM	mM	μS/cm			
Kasumigaura	1.38	3,060	770	0.030	2.2	0.88	0.83	0.08	0.44	0.2	0.86	0.12	0.5	0.11	92	Lake Kasumigaura in Ibaraki, Japan	24 August 2010	SPAC10, PAC10
Hakucho-10	1.24	2,660	710	0.048	3.9	0.88	0.83	0.08	0.44	0.2	0.86	0.12	0.5	0.11	92	Lake Hakucho, Hokkaido, Japan	25 September 2010	
Inba	1.46	3,060	990	0.032	2.2	1.54	0.83	0.08	0.44	0.2	0.86	0.12	0.5	0.11	92	Lake Inba, Chiba, Japan	18 September 2009	
Chibaberi-09	1.65	2,050	1,170	0.082	5.0	1.22	0.83	0.08	0.44	0.2	0.86	0.12	0.5	0.11	92	Chibaberi River, Hokkaido, Japan	17 September 2009	
Chibaberi-10	1.43	1,750	840	0.060	4.2	1.11	0.83	0.08	0.44	0.2	0.86	0.12	0.5	0.11	92	Chibaberi River, Hokkaido, Japan	2 December 2010	
SFA-10	1.60	2,690	1,300	0.068	4.3	1.02	0.83	0.08	0.44	0.2	0.86	0.12	0.5	0.11	92	Suwannee River fulvic acid (International Humic Substance Society)		
SHA-10	1.61	3,580	1,280	0.091	5.7	1.34	0.83	0.08	0.44	0.2	0.86	0.12	0.5	0.11	92	Suwannee River humic acid (International Humic Substance Society)		
OFW-10	0.0	—	—	0.000	—	0.99	0.83	0.08	0.44	0.2	0.86	0.12	0.5	0.11	92			
Hakucho-08	1.54	1,410	670	0.034	2.2	1.03	0.34	0.21	0.07	0.03	0.26	0.04	0.17	0.2	86	Lake Hakucho, Hokkaido, Japan	7 November 2008	SPAC08, PAC08
SFA-08	1.38	2,690	1,300	0.066	4.8	1.28	0.34	0.21	0.07	0.03	0.26	0.04	0.17	0.2	86	Suwannee River fulvic acid (International Humic Substance Society)		
SHA-08	1.51	3,580	1,280	0.092	6.1	1.00	0.34	0.21	0.07	0.03	0.26	0.04	0.17	0.2	86	Suwannee River humic acid (International Humic Substance Society)		
OFW-08	0.0	—	—	0.000	—	0.91	0.34	0.21	0.07	0.03	0.26	0.04	0.17	0.2	86			

Table 3S. Freundlich isotherm constants and exponents for MIB in OFW

	SPAC-10	PAC-10
K_M (nmol/mg)/(nmol/L)$^{1/n_M}$	4.44 (4.14 ~ 4.76)*	3.53 (3.37 ~ 3.70)
$1/n_M$ (dimensionless)	0.466 (0.406 ~ 0.527)	0.451 (0.411 ~ 0.492)
	SPAC-08	PAC-08
K_M (nmol/mg)/(nmol/L)$^{1/n_M}$	5.42 (4.85 ~ 6.06)	4.36 (3.88 ~ 4.90)
$1/n_M$ (dimensionless)	0.475 (0.409 ~ 0.540	0.510 (0.431 ~ 0.589)

* Values in parentheses represent 95% confidence interval ranges

Table 4S. Freundlich isotherm constants [K_M^* (nmol/mg)/(nmol/L)$^{1/n_M}$] obtained from MIB adsorption isotherm data collected in NOM-containing waters (from equation 4).

	SPAC-10	PAC10
Kasumigaura	0.71	0.56
Hakucho-10	0.76	0.61
Inba	1.37	1.03
Chibaberi-09	1.56	1.26
Chibaberi-10	1.15	0.99
SFA-10	1.20	0.98
SHA-10	1.84	0.97
	SPAC-08	PAC08
Hakucho-08	0.68	0.63
SFA-08	1.43	1.39
SHA-08	2.25	1.84

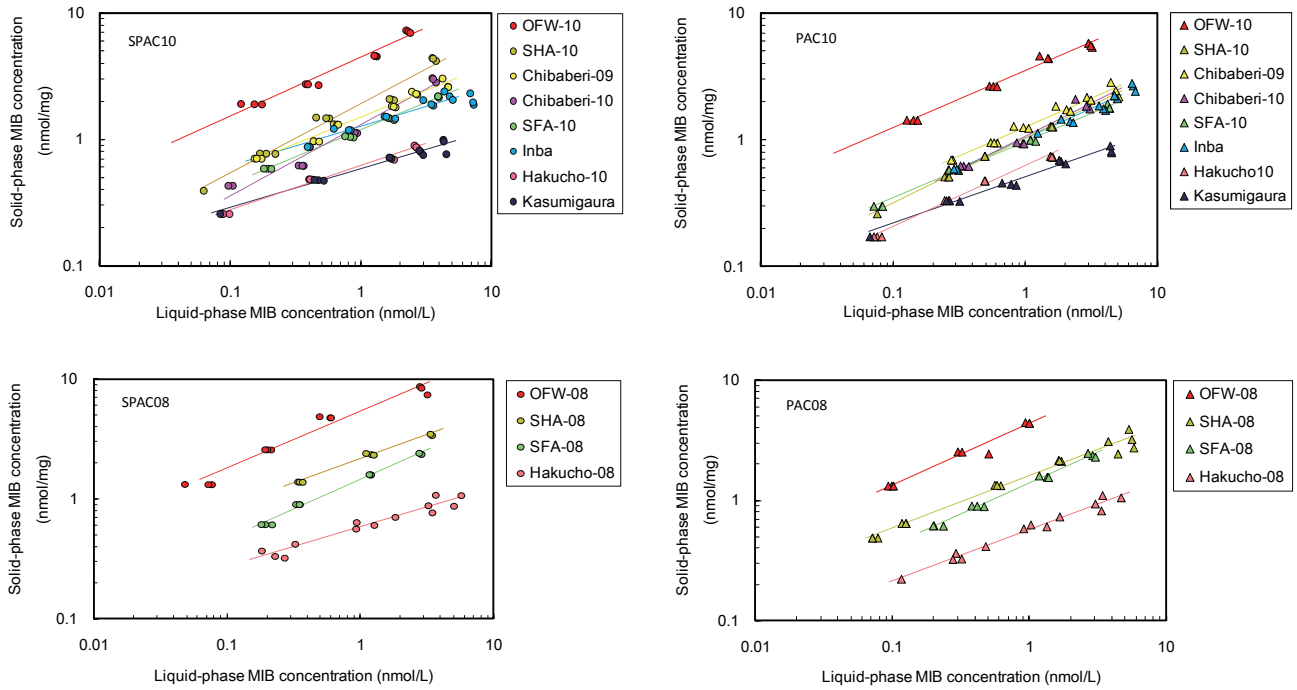

Figure 1S. MIB adsorption isotherms on SPAC and PAC (lines represent Freundlich isotherm model fits).

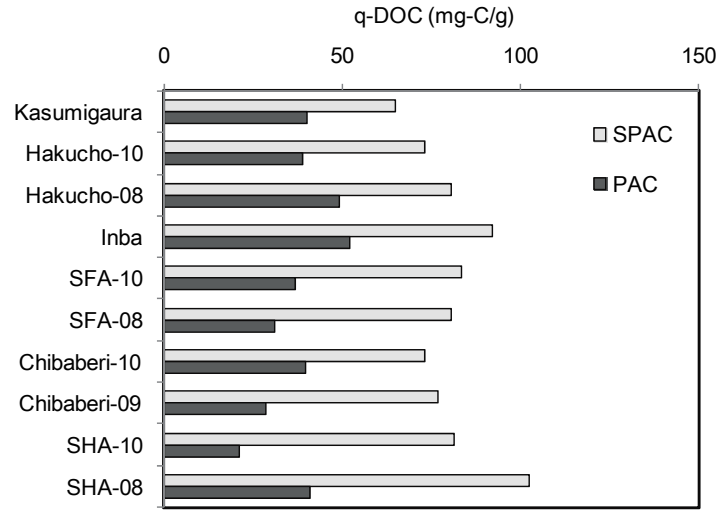

Figure 2S. DOC loadings at a carbon dose of 8 mg/L.

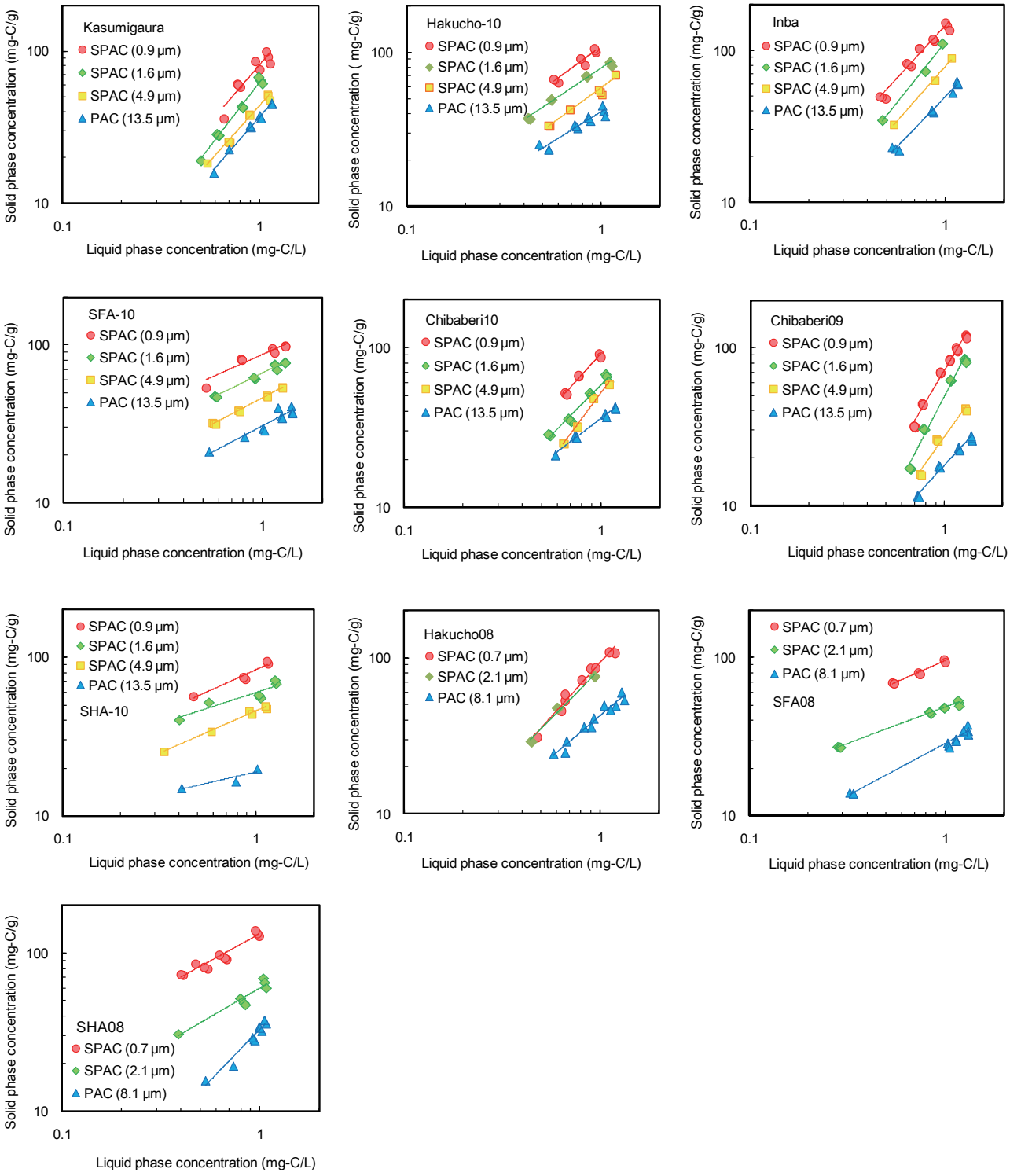

Figure 3S. DOC adsorption isotherms. Lines represent Freundlich isotherm model fits.

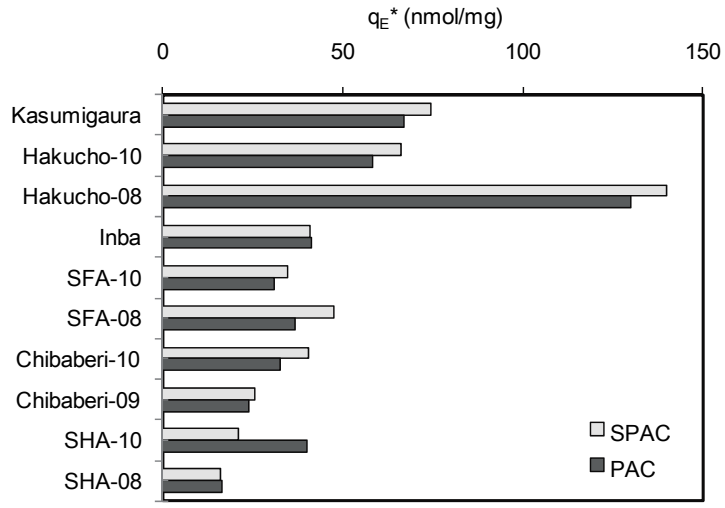

Figure 4S Pseudo solid-phase concentrations of the competing NOM fraction (q_E^*) at a carbon dose of 8 mg/L.

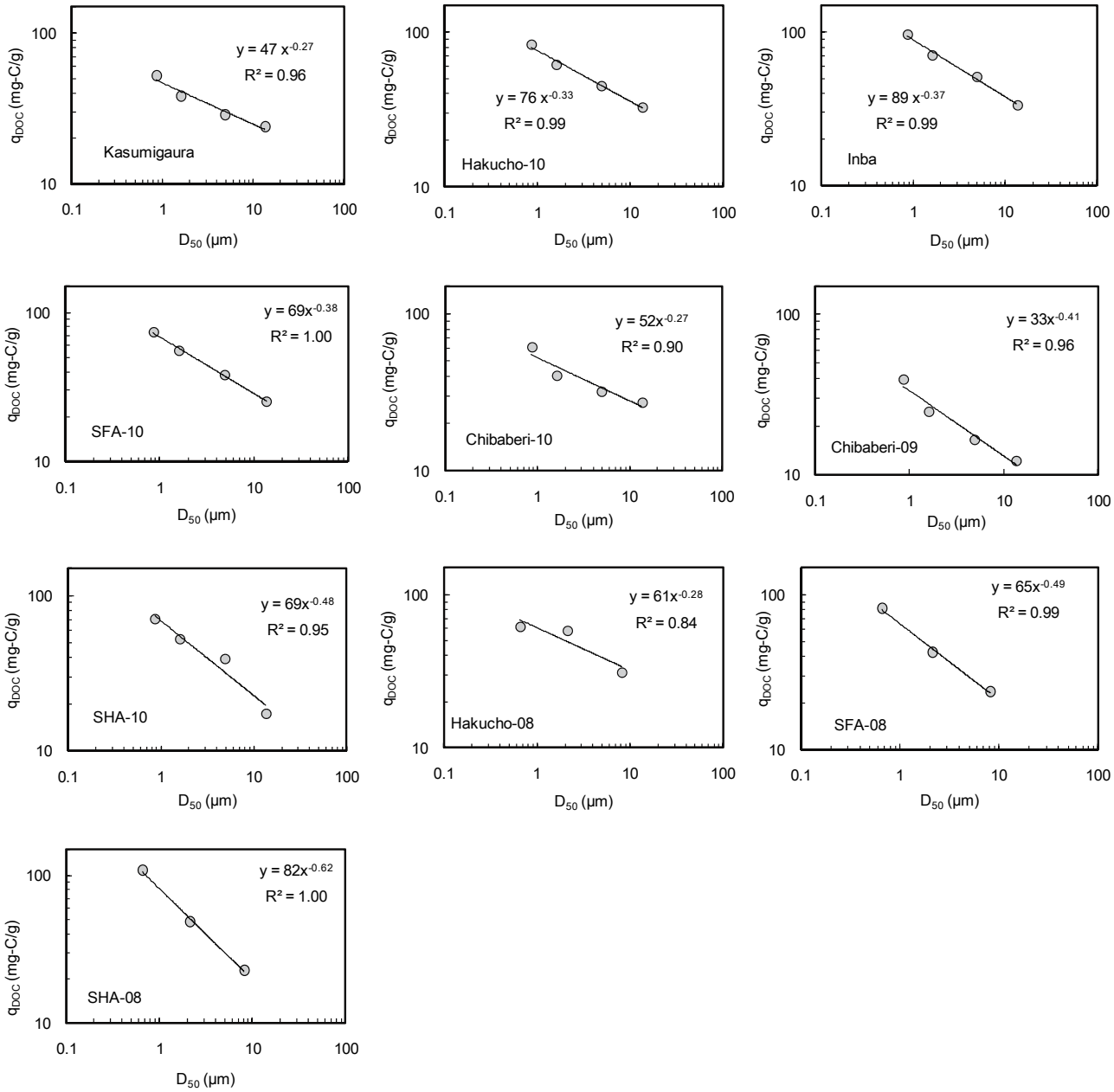

Figure 5S. Plots of q_{DOC} as a function of median carbon diameter (D_{50}). Values of q_{DOC} were calculated for the carbon dose, at which 50% of the initial aqueous-phase DOC concentration (1.5 mg-C/L) was adsorbed.

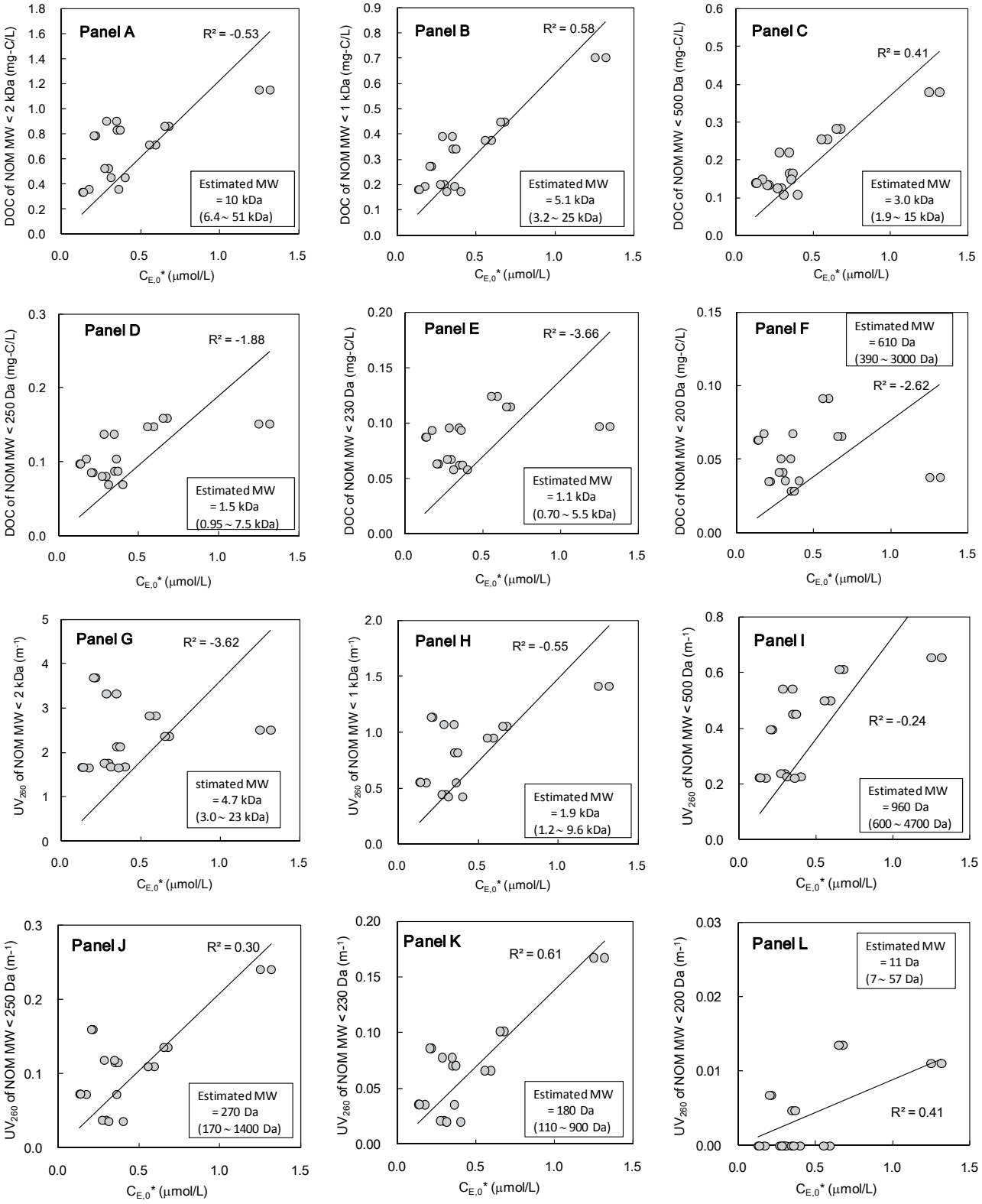

Figure 6S. Relationship between the concentration of a NOM fraction with a molecular weight smaller than indicated in the y-axis label and the competing NOM concentration ($C_{E,0}^*$). Concentrations of NOM fractions were obtained from size-exclusion chromatograms. $C_{E,0}^*$ values were estimated from MIB isotherms by using equations (3)-(6). Coefficients of determination (R^2) were determined from 1-SSreg/SStot, where SSreg is the sum of squares of the residuals around the regression line with an intercept of 0, and SStot is the sum of squares of the residuals around a horizontal line representing the mean mass concentration or absorbance value of the data shown in each panel (Motulsky and Christopoulos, 2004).